

## Synthesis and Application of Bimetallic Zinc(II) Phenoxy-Imine Complexes as Initiators for Production of Lactide Polymers

Alana L. C. Oliveira,<sup>a</sup> Leonardo C. Ferreira,<sup>a</sup> Marcos L. Dias,<sup>\*a</sup> Rodrigo S. Bitzer,<sup>b</sup>  
Marco A. C. Nascimento,<sup>b</sup> Maria de Fátima V. Marques<sup>a</sup> and Laura Crociani<sup>c</sup>

<sup>a</sup>Instituto de Macromoléculas Professora Eloisa Mano (IMA),  
Universidade Federal do Rio de Janeiro, 21941-598 Rio de Janeiro-RJ, Brazil

<sup>b</sup>Instituto de Química, Universidade Federal do Rio de Janeiro, 21044-020 Rio de Janeiro-RJ, Brazil

<sup>c</sup>Materia Condensata e di Tecnologie per l'Energia, Consiglio Nazionale Delle Ricerche,  
35127 Padova, Italy

This article reports the synthesis of two bimetallic zinc(II) complexes containing phenoxy-imine ligands and their application as initiators of ring opening polymerization (ROP) of L-lactide (LA). The phenoxy-imine ligands were obtained from salicylaldehyde derivatives and 2,3,5,6-tetramethylphenylenediamine, yielding two bidentate regions *per* ligand. The reactions of both phenoxy-imine ligands with ZnEt<sub>2</sub> in the presence of *n*-BuOH afforded [Zn<sub>2</sub>(L1)(OBu)<sub>2</sub>] and [Zn<sub>2</sub>(L2)(OBu)<sub>2</sub>], which were characterized by elemental analysis, Fourier transform infrared (FTIR) and <sup>1</sup>H nuclear magnetic resonance (NMR) spectroscopy. In addition, the geometries of both complexes were investigated by DFT (B3LYP/LACVP\*\*) calculations. [Zn<sub>2</sub>(L1)(OBu)<sub>2</sub>] and [Zn<sub>2</sub>(L2)(OBu)<sub>2</sub>] were tested as initiators of ROP of LA at 180 °C using different LA/Zn molar ratios, namely 500, 1000 and 2500. Both complexes showed good activity, resulting in conversions up to 96% in 2 h. The poly-LLA exhibited average molecular weight (M<sub>w</sub>) ranging from 45,000-92,000, relatively low polydispersity (M<sub>w</sub>/M<sub>n</sub> = 1.6-2.0) and high stereoregularity with melting temperature T<sub>m</sub> = 164 °C.

**Keywords:** L-lactide, zinc complex, phenoxy-imine, polymerization, DFT calculations

### Introduction

The manufacture of lactide polymers has been pursued due to their biodegradability and biocompatibility. Polylactide (PLA) and their copolymers are important polyesters. They are versatile macromolecules that can be used in biomedical areas, such as prostheses and implants, and in the pharmaceutical industry as components of drug delivery systems, besides their applications in packaging.<sup>1</sup>

An effective way to produce these polymers involves ring-opening polymerization (ROP) of lactides (LAs). Several methodologies are available for such reactions. However, the most commonly used methodology exploits coordination-insertion pathways, since they allow the production of higher molecular weight polymers exhibiting low polydispersity. Furthermore, these reactions offer a high degree of polymer structure and tacticity controls.<sup>2,3</sup> ROP of

lactide monomers requires the use of catalysts (initiators) that may be cationic, anionic or neutral coordination complexes and should provide a rapid polymerization with adequate control of polymer features.<sup>3,4</sup> There is a great number of metal-based catalysts able to perform ROP reactions via coordination-insertion mechanism. However, some of these catalysts are toxic and difficult to remove from the reaction mixtures, preventing applications of the resulting polymers in biomedical and pharmaceutical areas.<sup>2,5</sup>

Zinc(II) complexes are ubiquitous in catalysis, from enzymatic transformations to organic synthesis. In effect, zinc(II) complexes have been employed as initiators to produce PLA by ROP reactions. In addition to being a soft Lewis acid, zinc is a biocompatible metal, providing less poisonous residues in the produced polymers if compared to other metals. Among other features, Zn-based initiators allow a high control over polymer tacticity, thus producing polymers with high stereoregularity.<sup>5-7</sup> Although different coordination compounds could be used as catalysts for LA

\*e-mail: mldias@ima.ufrj.br

polymerization, little is known about the influence of their structures and electronic properties on PLA production.<sup>8,9</sup> In this respect, we have been interested in the synthesis of phenoxy-imine ligands capable of simultaneously coordinating two metal atoms. This kind of ligand can furnish bimetallic Zn-based initiators containing two metal centers close to each other, which can act in a synergic fashion during the polymerization reaction.

In this work, we report the synthesis, spectroscopic characterization and DFT (density functional theory) study of two new bimetallic zinc(II) complexes containing phenoxy-imine ligands, and their application as initiators of ROP of L-lactide aiming to correlate the influence of the initiator structure on the thermal properties of the produced poly(L-lactic acid).

## Experimental

### Materials

The syntheses of the bimetallic zinc(II) complexes and the polymerization reactions were carried out under inert atmosphere (dry N<sub>2</sub>) using Schlenk-type glassware and glove bags. Toluene was dried over sodium-benzophenone under N<sub>2</sub>. 3,5-Diiodine-2-hydroxybenzaldehyde and 5-methyl-2-hydroxybenzaldehyde (Aldrich), ZnEt<sub>2</sub> 15% solution in hexane (Akzo Nobel), and EtOH were purchased from commercial sources and used as received. *n*-BuOH (Aldrich) was dried under molecular sieves. L-Lactide (Purac) was recrystallized from dry toluene prior to use.

### Ligands and complexes characterization

Nuclear magnetic resonance (NMR) spectra were recorded on a Varian Mercury VX (300 MHz, 25 °C) spectrometer using CDCl<sub>3</sub>. Fourier transform infrared (FTIR) analyses were carried out on a Frontier FT-IR/FIR spectrometer using the technique of attenuated total reflectance (ATR). Melting points were determined using a Quimis melting point apparatus (model 0340513) with controlled heating. Elemental analyses were performed in a HANAU Elementary Vario Micro cube.

### Lactide polymerization

The activity of **C1** and **C2** was investigated in the bulk polymerization of L-lactide using molar monomer/initiator ratios LA/Zn = 500, 1000 and 2500. The mixture of the desired zinc initiator and L-lactide was prepared in a Schlenk flask under nitrogen atmosphere and the polymerization was carried out by heating the mixture at 180 °C for 2 h,

after which the reaction medium was quenched by cooling it to room temperature.<sup>18</sup> Subsequently, the solid product was dissolved in chloroform and the polymer precipitated from ethanol. The isolated polymer was dried under vacuum at 50 °C.

### Polymer characterization

NMR spectra were recorded in a Varian Mercury VX-300 NMR spectrometer operating at 75 MHz (<sup>13</sup>C) (25 °C) using CDCl<sub>3</sub>. Gel permeation chromatography (GPC) was carried out in a Shimadzu LC 20 instrument equipped with a set of two Phenogel columns and a RID-20A differential index detector. GPC analyses were performed using chloroform as eluent at 1 mL min<sup>-1</sup> and 25 °C. A calibration curve using ten polystyrene standards was used for molecular weight determination by the Shimadzu software. Thermal properties of the polymers were determined by differential scanning calorimetry (DSC) using a TA Q1000 calorimeter with a heating and cooling rate of 10 °C min<sup>-1</sup> from -10 to 200 °C under nitrogen flow. Values of glass transition (T<sub>g</sub>), crystallization temperature on heating (cold crystallization, T<sub>cc</sub>) and melting temperature (T<sub>m</sub>) were obtained from a second heating after a quenching run. The crystallization temperature on cooling (T<sub>c</sub>) was recorded in a cooling run after the second heating run. Thermogravimetric analyses (TGA) were performed with a TA TGA Q500 Thermo analyzer. Measurements were carried out under nitrogen at a heating rate of 20 °C min<sup>-1</sup> up to 700 °C with a gas flow rate of 20 mL min<sup>-1</sup>.

### Synthesis of L1

**L1** was synthesized using a modified literature procedure.<sup>10-13</sup> An ethanolic solution (15 mL) of 3,5-diiodine-2-hydroxybenzaldehyde (1.244 g, 2 mmol) was added dropwise to an ethanolic solution (15 mL) of 2,3,5,6-tetramethylphenylenediamine (0.164 g, 1 mmol). The reaction mixture was refluxed for 3 h and then stirred overnight at room temperature. Subsequently, the resulting yellow solution was cooled, affording a yellow precipitate, which was filtered off and washed with hexane. Yield: 62%; mp > 300 °C; elemental analysis for C<sub>24</sub>H<sub>20</sub>N<sub>2</sub>O<sub>2</sub>I<sub>4</sub> (anal. calcd. (found)): C, 32.89 (32.70); H, 2.28 (2.45), N: 3.19 (3.30); IR (KBr, ± 4 cm<sup>-1</sup>) ν / cm<sup>-1</sup> 3433 (νO-H), 2916 (νC-H, aromatic), 1617 (νC=N, imine), 1545 and 1432 (νC=C, aromatic), 1277 (νC-N), 1155 and 1064 (νC-O, phenol), 645 (νC-I); <sup>1</sup>H NMR (300 MHz, CDCl<sub>3</sub>, 25 °C) δ 8.23 (s, 2H, CH=N), 7.24-7.05 (m, 4H, ArH), 2.35 (s, 12H, CH<sub>3</sub>).

## Synthesis of **L2**

**L2** was similarly synthesized from 5-methyl-2-hydroxybenzaldehyde (0.800 g, 2 mmol) and 2,3,5,6-tetramethylphenylenediamine (0.164 g, 1 mmol). Yield: 60%; mp 271-272 °C; elemental analysis for C<sub>26</sub>H<sub>28</sub>N<sub>2</sub>O<sub>2</sub> (anal. calcd. (found)): C, 78.01 (78.40); H, 7.00 (6.89); N, 7.00 (7.20); IR (ATR, ± 4 cm<sup>-1</sup>) ν / cm<sup>-1</sup> 3432 (νO–H); 2917 (νC–H, aromatic), 1625 (νC=N, imine), 1593 and 1491 (νC=C, aromatic), 1280 (νC–N), 1068 (νC–O, phenol); <sup>1</sup>H NMR (300 MHz, CDCl<sub>3</sub>, 25 °C) δ 8.16 (s, 2H, CH=N), 8.09-7.62 (m, 6H, ArH), 5.4 (m, 2H, –OH, phenol), 2.14 (s, 18H, CH<sub>3</sub>).

## Synthesis of [Zn<sub>2</sub>(L1)(OBu)<sub>2</sub>] (**C1**)

**C1** was prepared using a modified literature procedure.<sup>14-17</sup> In a 25 mL Schlenk flask, 15% hexane solution of ZnEt<sub>2</sub> (0.20 mL, 0.22 mmol) was added dropwise to a solution of **L1** (0.100 g, 0.11 mmol) in dry toluene (10 mL) at 0-4 °C (**L1**/ZnEt<sub>2</sub> molar ratio = 1:2). The reaction mixture was stirred overnight at room temperature. After this period, 0.02 mL of *n*-BuOH was added, maintaining the mixture under stirring for additional 3 h. The greenish-yellow solid formed was washed three times with dry toluene and dried under vacuum. Yield: 80%; mp > 300 °C; elemental analysis for Zn<sub>2</sub>C<sub>32</sub>H<sub>36</sub>N<sub>2</sub>O<sub>4</sub>I<sub>4</sub> (anal. calcd. (found)): C, 33.38 (33.75); H, 3.13 (3.27); N, 2.43 (2.60); IR (KBr, ± 4 cm<sup>-1</sup>) ν / cm<sup>-1</sup> 2921 (νC–H, aromatic), 1598 (νC=N, imine), 1489 and 1433 (νC=C, aromatic), 1214 (νC–N), 1142-1065 (νC–O, phenol), 686 (νC–I); <sup>1</sup>H NMR (300 MHz, CDCl<sub>3</sub>, 25 °C) δ 7.26 (m, 4H, ArH), 2.34-2.00 (s, 4H, –O–CH<sub>2</sub>–, butylalcohol), 1.51 (s, 12H, Ar–CH<sub>3</sub>), 1.26 (s, 4H, –CH<sub>2</sub>–, butylalcohol), 0.89 (s, 4H, –CH<sub>2</sub>–, butylalcohol) and 0.07 (s, 6H, CH<sub>3</sub>, butylalcohol).

## Synthesis of [Zn<sub>2</sub>(L2)(OBu)<sub>2</sub>] (**C2**)

**C2** was similarly prepared from **L2** (0.100 g, 0.25 mmol) and 15% hexane solution of ZnEt<sub>2</sub> (0.41 mL, 0.50 mmol) (**L2**/ZnEt<sub>2</sub> molar ratio = 1:2). Yield: 85%; mp > 300 °C; elemental analysis for Zn<sub>2</sub>C<sub>34</sub>H<sub>44</sub>N<sub>2</sub>O<sub>4</sub> (anal. calcd. (found)): C, 60.46 (60.80); H, 6.52 (6.99); N, 4.15 (4.57); IR (ATR, ± 4 cm<sup>-1</sup>) ν / cm<sup>-1</sup> 2920 (νC–H, aromatic), 1595 (νC=N, imine), 1531 and 1467 (νC=C, aromatic), 1321 (νC–N), 1069 (νC–O, phenol); <sup>1</sup>H NMR (300 MHz, CDCl<sub>3</sub>, 25 °C) δ 8.23 (s, 2H, CH=N), 7.30 (m, 6H, ArH), 2.34 (s, 4H, –O–CH<sub>2</sub>–, butylalcohol), 2.13 (s, 18H, Ar–CH<sub>3</sub>), 1.50 (s, 4H, –CH<sub>2</sub>–, butylalcohol), 1.3 (s, 4H, –CH<sub>2</sub>–, butylalcohol), 0.08 (s, 6H, CH<sub>3</sub>, butylalcohol).

## DFT calculations

All calculations were carried out with JAGUAR 7.9 using an energy convergence criterion of 1.00 × 10<sup>-8</sup> hartree.<sup>19</sup> Gas-phase geometry optimizations were performed without constraints using the B3LYP hybrid functional along with the LACVP\*\* basis set.<sup>20</sup> The vibrational frequencies of each optimized geometry were evaluated at the same level of calculation and verified to be real.<sup>21</sup> An excellent agreement between experimental and calculated frequencies was obtained.

## Results and Discussion

### Ligands and complexes

The condensation reaction of salicylaldehyde derivatives with anilines constitutes an ordinary method for the preparation of phenoxy-imines and was used in this work to prepare two bidentate ligands (**L1** and **L2**). **L1** and **L2** were synthesized in high yields according to a modified literature procedure.<sup>14-17,22</sup> Complexes **C1** and **C2** (Figure 1) were also obtained in high yields. The structures of these ligands allow the coordination of two zinc(II) centers while the vast majority of the phenoxy-imine ligands coordinate to only one metal.

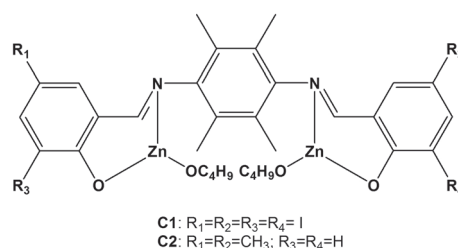


**Figure 1.** Structural formulas for **C1** and **C2**.

In the IR spectra of **L1** and **L2** (Figures 2 and 3), ν(OH) bands of weak intensity lie at about 3430 cm<sup>-1</sup>, while strong ν(C=N) bands occur at about 1620 cm<sup>-1</sup>. After coordination of zinc(II), the ν(C=N) and ν(C=C) bands were shifted to lower wavenumbers with respect to **L1** and **L2** (Figures 2 and 3).<sup>23</sup> The presence of ν(O–H) bands after complexation may be ascribed to residual solvent (*n*-BuOH) molecules or complex degradation.<sup>24,25</sup> Figures 4 and 5 illustrate the <sup>1</sup>H NMR spectra of **C1** and **C2**, respectively. Aromatic and aliphatic <sup>1</sup>H signals occur in the expected regions.

### DFT calculations

Two conformers were considered for each zinc(II) initiator (Figure 6). At the B3LYP/LACVP\*\* level of

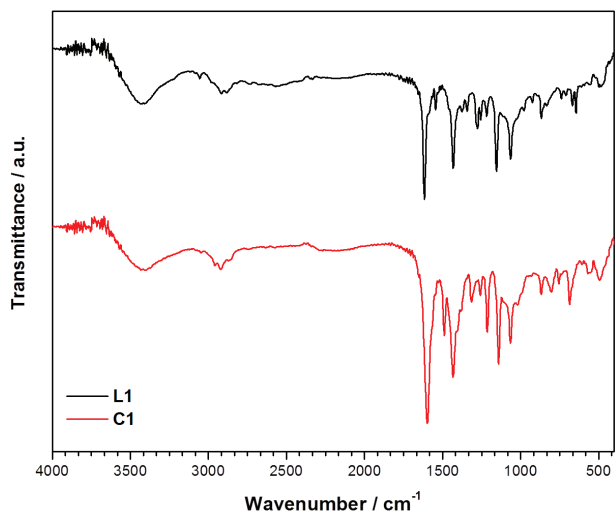


Figure 2. FTIR (KBr) spectra of L1 and C1.

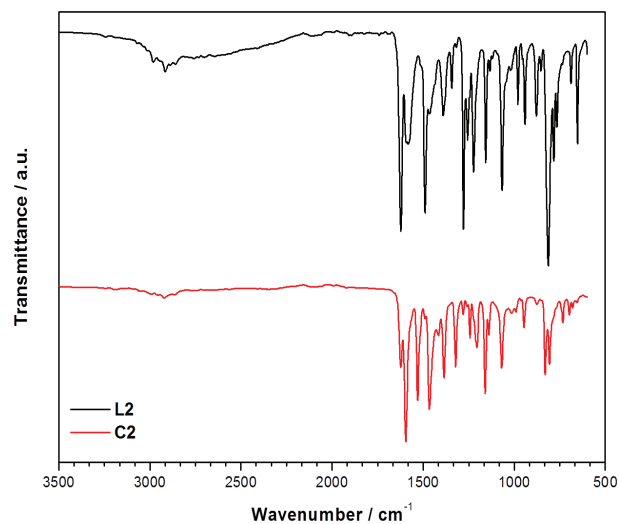
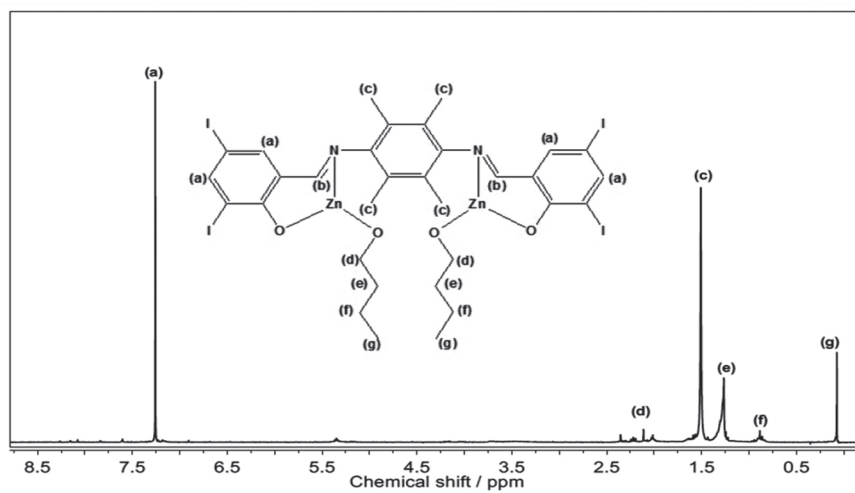
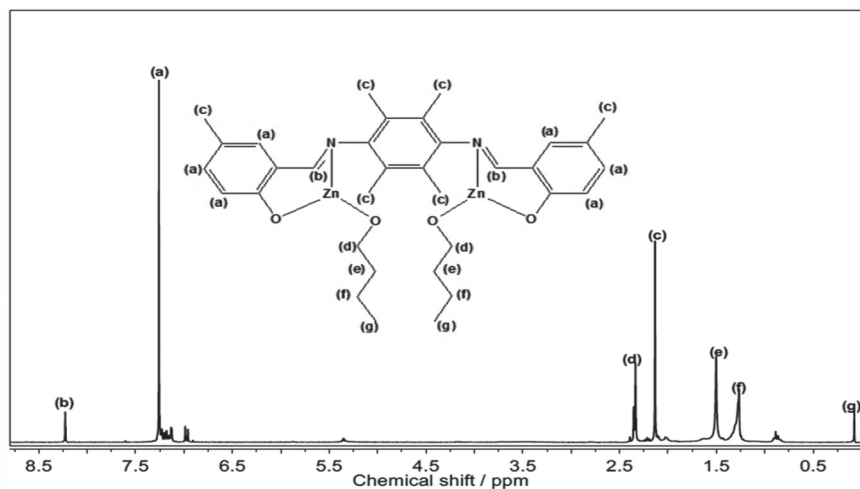
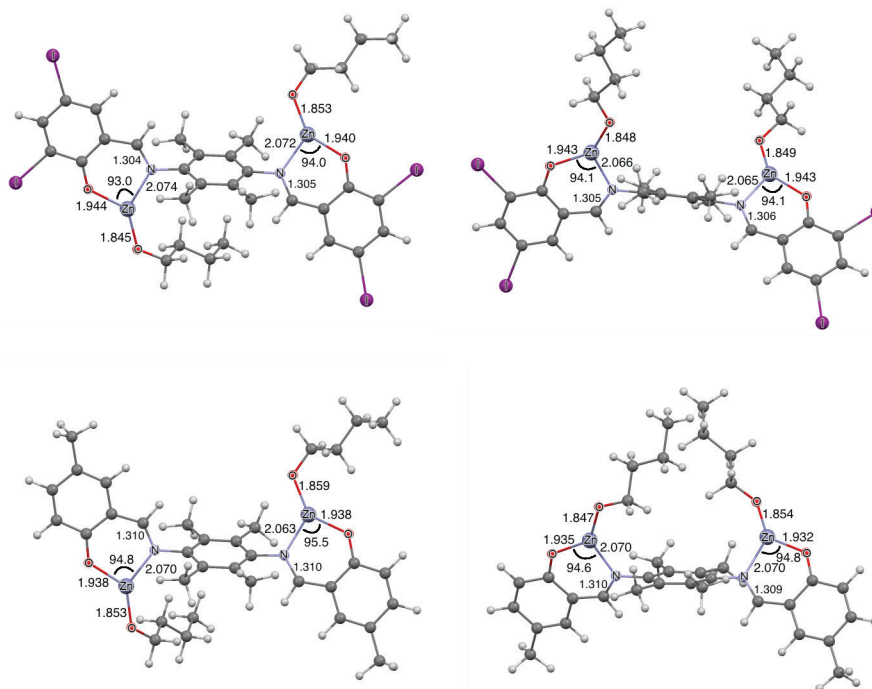


Figure 3. FTIR (ATR) spectra of L2 and C2.

Figure 4.  $^1\text{H}$  NMR spectrum (300 MHz,  $\text{CDCl}_3$ ) of C1.Figure 5.  $^1\text{H}$  NMR spectrum (300 MHz,  $\text{CDCl}_3$ ) of C2.



**Figure 6.** Geometries of *anti*- and *syn*-**C1** (top) and *anti*- and *syn*-**C2** (bottom) optimized at the B3LYP/LACVP\*\* level of calculation. Bond distances are given in Å and angles in degrees.

calculation, the self-consistent field (SCF) energy difference between *anti*-**C1** and *syn*-**C1** is very small (0.7 kcal mol<sup>-1</sup>), whereas *anti*-**C2** is only 1.8 kcal mol<sup>-1</sup> more stable than *syn*-**C2**. Based on these results, both initiators are likely to operate as a mixture of isomers in the reaction conditions. Figure 6 shows that **C1** and **C2** exhibit three-coordinate zinc(II) centers in the expected trigonal planar coordination environment. Moreover, the Zn–O<sub>OBu</sub> bond is shorter than Zn–O<sub>OPh</sub> regardless of the isomer. Our DFT results suggest that both **C1** and **C2** operate via imine-phenoxide-assisted coordination-insertion ROP mechanism.

### Polymerization

**C1** and **C2** were evaluated regarding their activity to produce poly(L-lactide) from ROP of L-lactide (LLA) (Figure 7). Polymerizations were carried out using different

LLA/Zn molar ratios (500, 1000 and 2500) in 2 h at 180 °C. Polymer yield, number average molecular weight ( $M_n$ ), weight average molecular weight ( $M_w$ ) and polydispersity ( $M_w/M_n$ ) are presented in Table 1.

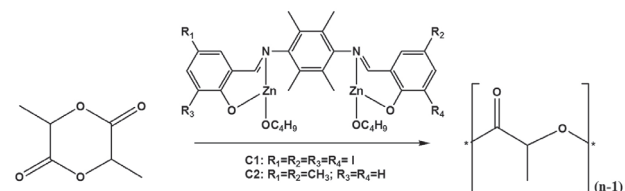


**Figure 7.** Polymerization of L-lactide catalyzed by **C1** and **C2**.

**C1** and **C2** are very effective initiators for bulk polymerization of L-lactide, producing poly(L-lactic acid) (PLLA) in good yields (between 71 and 96%) when reactions were performed at 180 °C for 2 h. For

**Table 1.** Polymerization of L-lactide with **C1** and **C2** at 180 °C for 2 h

Initiator	[LLA]/[Zn]	$M_n$	$M_w / (\text{g mol}^{-1})$	$M_w/M_n$	Yield / %
<b>C1</b>	500	40,800	66,600	1.63	95.8
	1000	46,000	82,000	1.78	96.0
	2500	50,100	92,200	1.84	86.7
<b>C2</b>	500	35,000	65,200	1.86	93.0
	1000	24,800	50,100	2.02	79.5
	2500	26,000	45,200	1.74	71.5

$M_n$ : number average molecular weight;  $M_w$ : weight average molecular weight;  $M_w/M_n$ : polydispersity.



both initiators, the yield increased as the LLA/Zn molar ratio decreased, attaining a maximum yield of 96% at LLA/Zn = 500. This behavior can be explained considering that at lower LLA/Zn ratios, the Zn concentration and consequently the number of active species are higher, increasing the polymerization rate. The PLLA obtained with these initiators showed relatively high molecular weight, with  $M_w$  varying from 45,200 to 92,200 g mol<sup>-1</sup>. It is important to highlight that the two complexes have different behavior depending on the influence of LLA/Zn ratio on the PLLA molecular weight. For **C1**, when LLA/Zn ratio decreases,  $M_w$  also decreases, while for **C2**, when LLA/Zn ratio decreases,  $M_w$  increases. This behavior might be related to the ligand structure, but it cannot be rationalized at the moment.

The polydispersity ( $M_w/M_n$ ) of the polymers ranges from 1.63 to 2.02, which is in the range expected for high molecular weight PLLA obtained by ROP with metal initiators.<sup>5</sup> **C1** produced polymers in higher yields, higher molecular weights and lower polydispersities as compared with **C2**.

As reported in literature, for many medical application a  $M_w$  of about 70,000 g mol<sup>-1</sup> is desired, for instance for preparation of electrospun scaffolds. Thus, the  $M_w$  obtained in this work is exactly in the desired range for some medical application.<sup>2,5</sup>

It is important to mention that the molecular weights were obtained by GPC. All PLLA samples showed monomodal GPC curves (not presented in this work), indicating that only one type of active species seems to be present during the polymerization reactions. According to our DFT results, each complex can exist as two stable isomers, *anti* and *syn*. Moreover, each complex has two

metallic centers capable of polymerizing LLA. In this regard, all active catalysts are likely to behave in a similar fashion during the catalysis, indicating that for each bimetallic initiator the metal centers are kinetically isolated from each other. Therefore, the differences in the polymer features obtained with **C1** and **C2** seem to be influenced by the stereoelectronic features of the phenoxy-imine ligands and should not be attributed to the different isomers that occur in the reaction mixture.

#### Microstructure of PLLA

The microstructures of the PLLA were studied by <sup>13</sup>C NMR spectroscopy. The <sup>13</sup>C NMR spectra of these polymers show three signals at 16, 68.5 and 169 ppm, attributed to methyl, methine and carbonyl groups, respectively.<sup>5,26-28</sup> The polymerization of L-lactide can produce a highly isotactic polymer if no side reactions, like racemization, take place during polymerization. Racemization reactions can be induced by the metal initiator and, in principle, it is influenced by the metal type and ligand structure, introducing D-lactyl units in the polymer structure. The presence of these isomeric units in the polymer backbone is manifested by the appearance of lateral side signals in the methine and carbonyl signals.<sup>18</sup> <sup>13</sup>C NMR spectra of these polymers (Figure 8) did not show any significant signals beside the peak of the carbonyl and methine regions, suggesting that L-D dyads are not present in significant amounts. Therefore, the PLLA polymer structures are highly stereoregular. Apparently, the different stereoelectronic attributes of **C1** and **C2** did not strongly affect the regularity of the produced PLLA, which are highly isotactic.

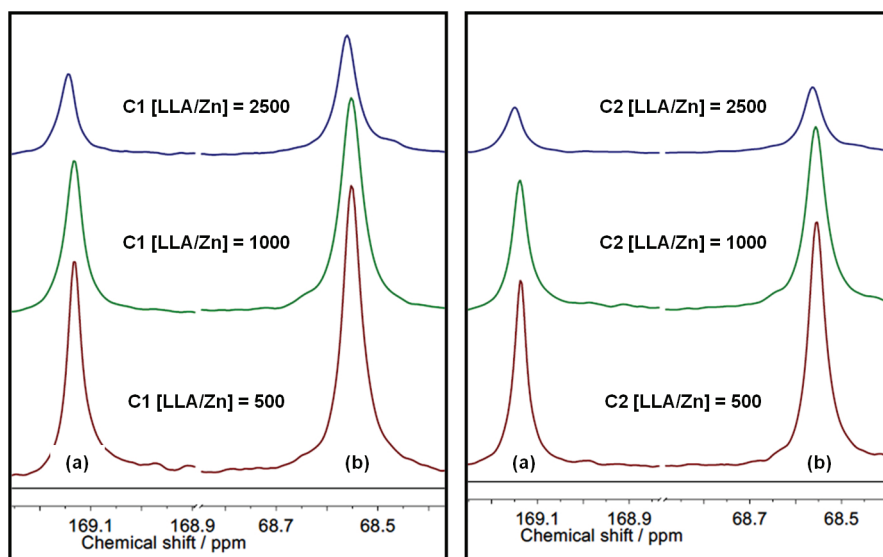


**Figure 8.** <sup>13</sup>C NMR spectra (75 MHz, CDCl<sub>3</sub>) of PLLA prepared with **C1** and **C2**: (a) carbonyl and (b) methine groups.

Powder X-ray diffraction (XRD) data were used to obtain information on the crystallinity of the resulting PLLA (Figures 9 and 10). From XRD, it is possible to infer that the initiators could produce highly crystalline polymers. It was not possible to identify by this technique any relation between the complex structure and the degree of crystallinity ( $X_c$ ) of the polymers, but it is possible to note that the intensity of the reflection at about  $17^\circ$  increased as LLA/Zn increased for **C1**, suggesting the influence of LLA/Zn in the polymer crystallinity. However, the tendency observed for **C1** was not reproduced for **C2**, since the crystallinity seems to decrease as the LLA/Zn ratio increased by considering the intensity of this reflection.

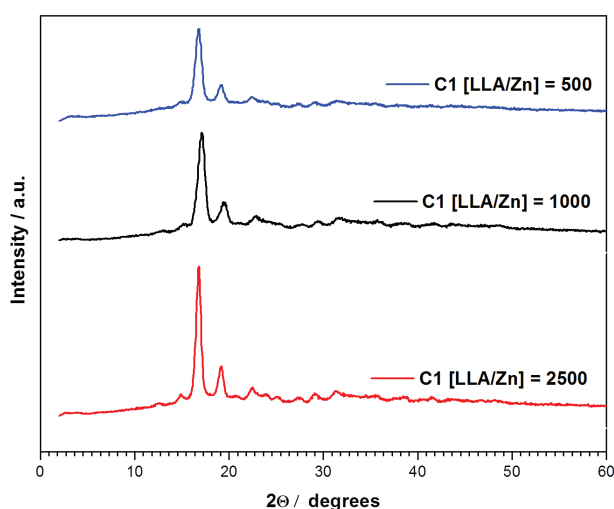


Figure 9. XRD curves for PLLA obtained from **C1**.

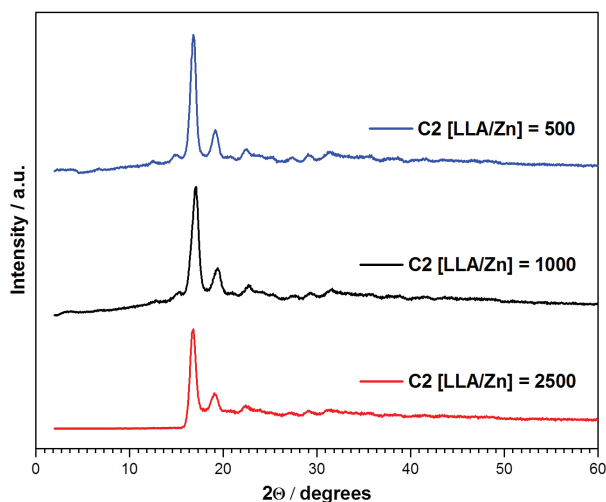


Figure 10. XRD curves for PLLA obtained from **C2**.

#### Thermal properties of PLLA

Figure 11 shows the DTG curves for the polymers obtained in this work. The results show that the PLLAs

obtained from **C1** exhibit the lowest temperature of maximum degradation rate  $T_{max}$ , considering the three LLA/Zn molar ratios. The PLLAs obtained from **C2** showed a remarkably higher  $T_{max}$  in the three LLA/Zn molar ratios. This demonstrates that the thermal property of PLLA was directly influenced by the structural and electronic variation of the ligands coordinated to  $Zn^{II}$ . It seems that the presence of iodine in the ligand **C1** structure led to less thermally stable PLLAs.

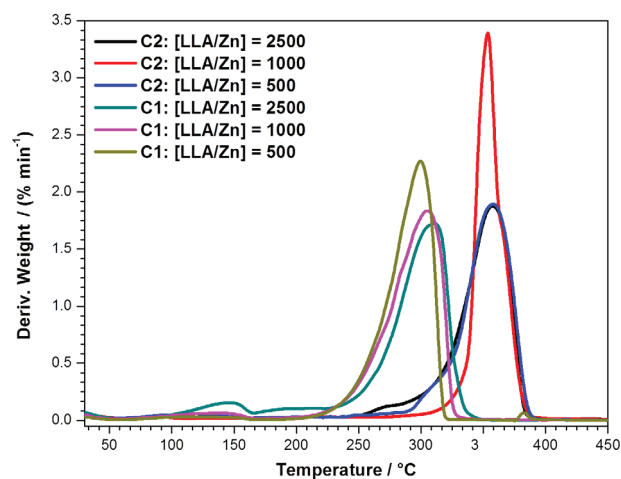


Figure 11. DTG curves for PLLAs obtained from **C1** and **C2**.

Table 2 summarizes the results of thermal stability for the polymers. When heated to  $700^\circ\text{C}$  under  $N_2$ , the PLLAs produced by using **C1** generated lower amount of residue than those prepared from **C2**. In addition, polymers prepared from **C1** showed lower thermal decomposition temperatures ( $T_{onset}$  and  $T_{max}$ ).

Table 2. Thermal degradation data for PLLAs obtained from **C1** and **C2**

Initiator	LLA/Zn	$T_{onset}$ / $^\circ\text{C}$	$T_{max}$ / $^\circ\text{C}$	Residue <sup>a</sup> / %
<b>C1</b>	500	270.1	120.7/299.7	2.2
	1000	270.1	136.8/304.9	4.2
	2500	276.9	148.5/312.5	0.5
<b>C2</b>	500	330.2	358.2	5.2
	1000	342.2	354.9	5.7
	2500	328.0	357.6	2.9

<sup>a</sup>Residue at  $700^\circ\text{C}$ .  $T_{onset}$  and  $T_{max}$ : thermal decomposition temperatures.

The transition temperatures and degree of crystallinity of the PLLAs were also determined by DSC. Figures 12 and 13 show the DSC heating run (second heating run after quenching) for PLLA obtained with catalysts **C1** and **C2**, respectively. The curves show 3 events: glass transition temperature ( $T_g$ ), crystallization temperature on heating (cold crystallization) ( $T_{cc}$ ), and melting transition temperature ( $T_m$ ).

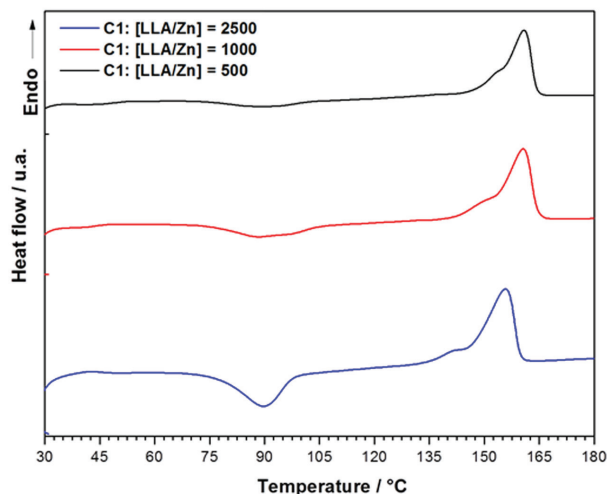


Figure 12. DSC curves of PLLA obtained with **C1** at different LLA/Zn molar ratios.

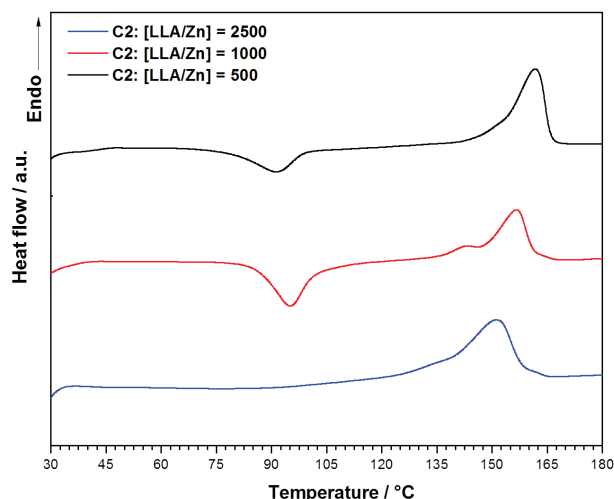


Figure 13. DSC curves of PLLA obtained with **C2** at different LLA/Zn molar ratios.

Table 3 lists the  $T_g$ ,  $T_m$ ,  $T_{cc}$ , and the degree of crystallinity ( $X_c$ ) of PLLAs obtained from the second heating run after a first melting of the samples to erase thermal history and quenching to obtain amorphous materials.

Table 3. Thermal properties of the PLLAs obtained by using **C1** and **C2** (second DSC heating run)

Initiator	LLA/Zn	$T_g$ / °C	$T_{cc}$ / °C	$T_m$ / °C	$X_c$ / %
<b>C1</b>	500	48.5	89.2	153.3/160.9	19.2
	1000	44.0	88.5	151.8/160.7	22.7
	2500	42.4	89.8	146.7/155.8	22.8
<b>C2</b>	500	43.0	89.4	150.3/163.8	28.7
	1000	41.8	95.2	148.3/156.7	18.9
	2500	42.2	85.5	130.1/151.3	33.6

$T_g$ : glass transition temperature;  $T_{cc}$ : crystallization temperature on heating (cold crystallization);  $T_m$ : melting transition temperature;  $X_c$ : degree of crystallinity.

Table 3 shows that the polymers obtained from **C1** and **C2** initiators display  $T_g$  values between 42 and 48 °C, which fall within the range usually found for PLLA (40–60 °C). Our values occur in the lower-bound of the expected range, which can be related to the molecular weight of these polymers as shown in Table 2. The literature reports that commercial high molecular weight PLLA ( $M_w$  above 150,000 g mol<sup>-1</sup>) has  $T_g$  around 60 °C. The polymers obtained in this work had  $M_w$  below 100,000 g mol<sup>-1</sup>. The  $T_g$  showed no significant variation with LLA/Zn ratio. The melting transition of the polymers showed a bimodal behavior with two visible peaks of  $T_m$  as described in Table 3. The peak at higher temperature varied from 151.3 to 163.8 °C, values in the range reported in literature (from 130 to 180 °C).<sup>29</sup> Regarding the degree of crystallinity ( $X_c$ ), almost no variation was observed relative to the variation of LLA/Zn ratio for the polymers synthesized from the **C1** initiator, whereas for **C2** the higher LLA/Zn ratio (lower Zn content) generated polymers with a higher degree of crystallinity. These two features, high molecular weights and crystallinity, of the polymers obtained from **C1** and **C2** make them appropriate for use as biomaterials.<sup>29,30</sup>

## Conclusions

Two bimetallic Zn<sup>II</sup> complexes (**C1** and **C2**) containing phenoxy-imine ligands were prepared and characterized by IR and <sup>1</sup>H NMR spectroscopy. Their molecular structures were optimized by DFT calculations at the B3LYP/LACVP\*\* level, which showed that both complexes have two stable isomers, *syn* and *anti*. **C1** and **C2** display the necessary features to act as initiators of lactide polymerization, showing good ROP activity in the bulk polymerization of L-lactide, resulting in the production of poly(L-lactic acid) (PLLA) with conversion up to 96%. The produced polymers are semi-crystalline materials and exhibit  $M_w$  up to 92,000 g mol<sup>-1</sup> and relatively low polydispersity in the polymerization condition used in this work. Based on the <sup>13</sup>C NMR and thermal data, we conclude that the polymers synthesized from **C1** and **C2** show high regularity. Apparently the difference between the structures of the ligands does not affect the regularity of the polymers obtained, but do directly affect their thermal stabilities. The polymers obtained from **C1** and **C2** exhibit high molecular weights and crystallinity which make them potential candidates for application as biomaterials.

## Acknowledgments

The authors are grateful to CNPq (310917/2014-0) and FAPERJ (E-26/201.304/2014) for financial support, and



CAPES (PNPD Program) and Project FP7-People-2011-IRSES-295262 (VAIKUTUS Project) for L. C. Ferreira Post-Doc fellowship.

## References

1. Xu, X.; Pan, X.; Tang, S.; Lv, X.; Li, L.; Wu, J.; Zhao, X.; *Inorg. Chem. Commun.* **2013**, *29*, 89.
2. Saha, T. K.; Mandal, M.; Chakraborty, D.; Ramkumar, V.; *New J. Chem.* **2013**, *37*, 949.
3. Idage, B. B.; Idage, S. B.; Kasegaonkar, A. S.; Jadhav, R. V.; *Mater. Sci. Eng. B* **2010**, *168*, 193.
4. Simic, V.; Spassky, N.; Hubert-Pfalzgraf, L. G.; *Macromolecules* **1997**, *30*, 7338.
5. Silvino, A. C.; Souza, K. S.; Dahmouche, K.; Dias, M. L.; *J. Appl. Polym. Sci.* **2012**, *124*, 1217.
6. Duan, R.; Gao, B.; Li, X.; Pang, X.; Wang, X.; Shao, H.; Chen, X.; *Polymer* **2015**, *71*, 1.
7. Bukhaltsev, E.; Frish, L.; Cohen, Y.; Vigalok, A.; *Org. Lett.* **2005**, *7*, 5123.
8. Deivasagayam, D.; Peruch, F.; *Polymer* **2011**, *52*, 4686.
9. Chuang, H.; Chen, H.; Ye, J.; Chen, Z.; Huang, P.; Liao, T.; Tsal, T.; Lin, C.; *Polym. Chem.* **2013**, *51*, 696.
10. Illingsworth, M. L.; Wang, W.; Hughes, K. A.; Terschak, J. A.; McCarny, J. P.; Stapleton, R. A.; Wagner, S. R.; Trotter, K. J.; Courtney, R. E.; Giacofei, R. A.; Jensen, A. J.; Moisa, M. S.; Browning, T. A.; Puchebner, B. E.; Theimer, C. A.; Chen, Y.; *Synth. React. Inorg. Met.-Org. Chem.* **2004**, *34*, 593.
11. Li, X.; Yang, T.; Wang, M.; Huo, L.; Li, Y.; *Yingyong Huaxue* **2013**, *30*, 43.
12. Bhunora, S.; Mugo, J.; Bhaw-Luximon, A.; Mapolie, S. J.; van Wyk, L.; Darkwa, J.; Nordlander, E.; *Appl. Organomet. Chem.* **2011**, *25*, 133.
13. Jones, M. D.; Davidson, M. G.; Keir, C. G.; Hughes, L. M.; Mahon, M. F.; Apperley, D. C.; *Eur. J. Inorg. Chem.* **2009**, *5*, 635.
14. Honrado, M.; Garcés, A.; Lara-Sánchez, A.; Rodríguez, A. M.; *Organometallics* **2012**, *31*, 4191.
15. Ghosh, S.; Chakraborty, D.; Ramkumar, V.; *Polym. Chem.* **2015**, *53*, 1474.
16. Honrado, M.; Otero, A.; Fernández-Baeza, J.; Sánchez-Barba, L. F.; Garcés, A.; Lara-Sánchez, A.; Martínez-Ferrer, J.; Sobrino, S.; Rodríguez, A. M.; *Organometallics* **2015**, *34*, 3196.
17. Kong, W. L.; Chai, Z. Y.; Wang, Z. X.; *Dalton Trans.* **2014**, *43*, 14470.
18. Dias, M. L.; Palermo, L. C.; Silvino, A. C.; *Macromol. Symp.* **2011**, *299/300*, 156.
19. Schrödinger; *JAGUAR Version 7.9*; LLC, New York, NY, 2011.
20. Becke, A. D.; *J. Chem. Phys.* **1993**, *98*, 5648.
21. Hay, P. J.; Wadt, W. R.; *J. Chem. Phys.* **1985**, *82*, 270.
22. Garcia-Valle, F. M.; Estivill, R.; Gallegos, C.; Cuenca, T.; Mosquera, M. E. G.; Taberner, V.; Cano, J.; *Organometallics* **2015**, *34*, 477.
23. Ferreira, L. C.; Filgueiras, C. A. L.; Visentim, L. C.; Bordinhão, J.; Hörner, M.; *Z. Anorg. Allg. Chem.* **2009**, *635*, 1225.
24. Chen, C.; Hung, C.; Chang, Y.; Peng, K.; Chen, M.; *J. Organomet. Chem.* **2013**, *738*, 1.
25. Silverstein, R. M.; Webster, F. X.; Kiemle, D. J.; *Spectrometric Identification of Organic Compounds*, 7<sup>th</sup> ed.; John Wiley & Sons: New Jersey, USA, 2005.
26. Suganuma, K.; Horiuchi, K.; Matsuda, H.; Cheng, H. N.; Aoki, A.; Asakura, T.; *Macromolecules* **2011**, *44*, 9247.
27. Suganuma, K.; Horiuchi, K.; Matsuda, H.; Cheng, H. N.; Aoki, A.; Asakura, T.; *Polym. J.* **2012**, *44*, 838.
28. Suganuma, K.; Matsuda, H.; Cheng, H. N.; Iwai, M.; Nonokawa, R.; Asakura, T.; *Polym. Test.* **2014**, *38*, 35.
29. Auras, R. A.; Harte, B.; Selke, S.; Hernandez, R.; *J. Plast. Film Sheeting* **2003**, *19*, 123.
30. Patel, H.; Bonde, M.; Srinivasan, G.; *Trends Biomater. Artif. Organs* **2011**, *25*, 20.

Submitted: April 4, 2017

Published online: July 10, 2017

